

Synthetic Variants of Mycolactone Bind and Activate Wiskott–Aldrich Syndrome Proteins

Anne-Caroline Chany,^{*,†} Romain Veyron-Churlet,[‡] Cédric Tresse,[†] Véronique Mayau,[‡] Virginie Casarotto,[†] Fabien Le Chevalier,[‡] Laure Guenin-Macé,[‡] Caroline Demangel,[‡] and Nicolas Blanchard^{*,§}

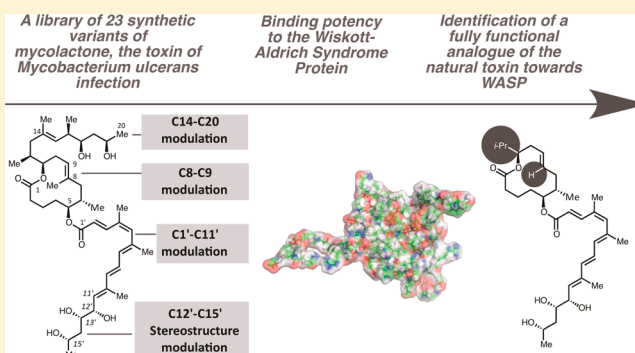
[†]Laboratoire de Chimie Organique et Bioorganique, Université de Haute-Alsace, ENSCMu, 3 Rue A. Werner, 68093 Mulhouse Cedex, France

[‡]Unité d'Immunobiologie de l'Infection, Institut Pasteur, CNRS URA1961, 25 Rue du Dr. Roux, 75724 Paris, France

[§]Laboratoire de Chimie Moléculaire, Université de Strasbourg, CNRS UMR 7509, Ecole Européenne de Chimie, Polymères et Matériaux, 25 Rue Becquerel, 67087 Strasbourg, France

S Supporting Information

ABSTRACT: Mycolactone is a complex macrolide toxin produced by *Mycobacterium ulcerans*, the causative agent of skin lesions called Buruli ulcers. Mycolactone-mediated activation of neural (N) Wiskott–Aldrich syndrome proteins (WASP) induces defects in cell adhesion underpinning cytotoxicity and disease pathogenesis. We describe the chemical synthesis of 23 novel mycolactone analogues that differ in structure and modular assembly of the lactone core with its northern and southern polyketide side chains. The lactone core linked to southern chain was the minimal structure binding N-WASP and hematopoietic homolog WASP, where the number and configuration of hydroxyl groups on the acyl side chain impacted the degree of binding. A fluorescent derivative of this compound showed time-dependent accumulation in target cells. Furthermore, a simplified version of mycolactone mimicked the natural toxin for activation of WASP in vitro and induced comparable alterations of epithelial cell adhesion. Therefore, it constitutes a structural and functional surrogate of mycolactone for WASP/N-WASP-dependent effects.



INTRODUCTION

Mycobacterium ulcerans infection causes a necrotizing skin disease called Buruli ulcer (BU), which affects a wide range of hosts including mammals, fishes, and frogs.^{1–5} Although first clinically diagnosed in man in 1948 by Australian researchers,⁶ it was only in 1999 that the exotoxin secreted by the causative organism, *Mycobacterium ulcerans*, was discovered by Small.^{7,8} Extensive multinuclear NMR experiments combined with chemical synthesis by Kishi^{9–12} finally led to the full characterization of a macrolide, named mycolactone A/B (Figure 1), which consists of a 8-undecenolide (C1–C11 fragment) substituted at C11 by a nine-carbon atom chain (C12–C20 northern fragment) and at C5 by a pentaenoic acid ester (C1'–C16' southern fragment).

The production of mycolactone is unique to *M. ulcerans* among human pathogens and underpins bacterial virulence. It is sufficient to induce Buruli ulcer (BU)-like lesions that are marked by an intriguing combination of tissue necrosis and lack of inflammation.¹³ Neural (N) Wiskott–Aldrich syndrome proteins (WASPs) is a key player in the ulcerative effects of mycolactone.¹⁴ Unlike its hematopoietic homolog WASP, N-WASP is ubiquitously expressed. Both proteins transduce

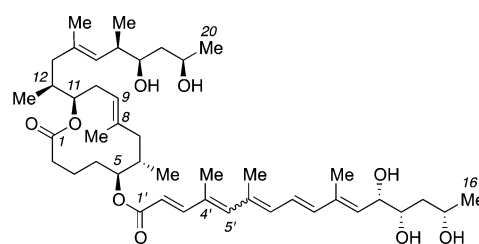


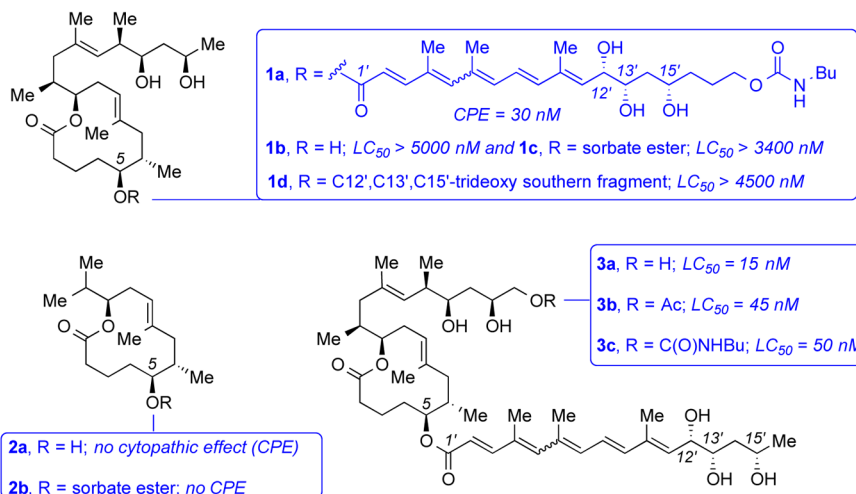
Figure 1. Chemical structure of mycolactone A/B, the exotoxin of *M. ulcerans*, as a Z - $\Delta^{4',5'}$ / E - $\Delta^{4',5'}$ = 60:40 dynamic equilibrium.

endogenous signals into dynamic remodeling of the actin cytoskeleton via interaction of their C-terminal verprolin-cofilin-acidic (VCA) domain with the Arp2/3 actin-nucleating complex.¹⁵ Mycolactone was shown to bind WASP and N-WASP selectively with 20–70 nM affinity, respectively. Binding triggered transition from an autoinhibited state, in which the VCA domain is sequestered, into an active state where released VCA can bind Arp2/3. In epithelial cells, mycolactone-induced

Received: June 10, 2014

Published: August 26, 2014

A. Mycolactone analogues by Kishi and Altmann



B. Mycolactone analogues by Blanchard

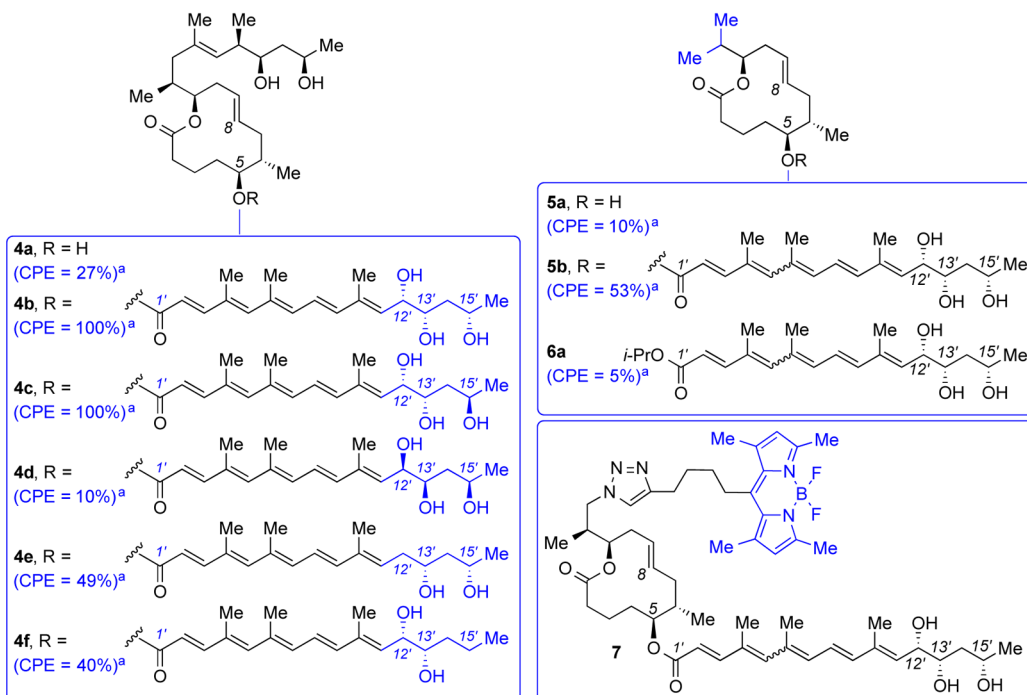


Figure 2. Mycolactone analogues by Kishi, Altmann, and Blanchard. Footnote letter in the figure indicates the following: ^aPercentage of cell rounding after 48 h of incubation with 10 μ M of product.³³

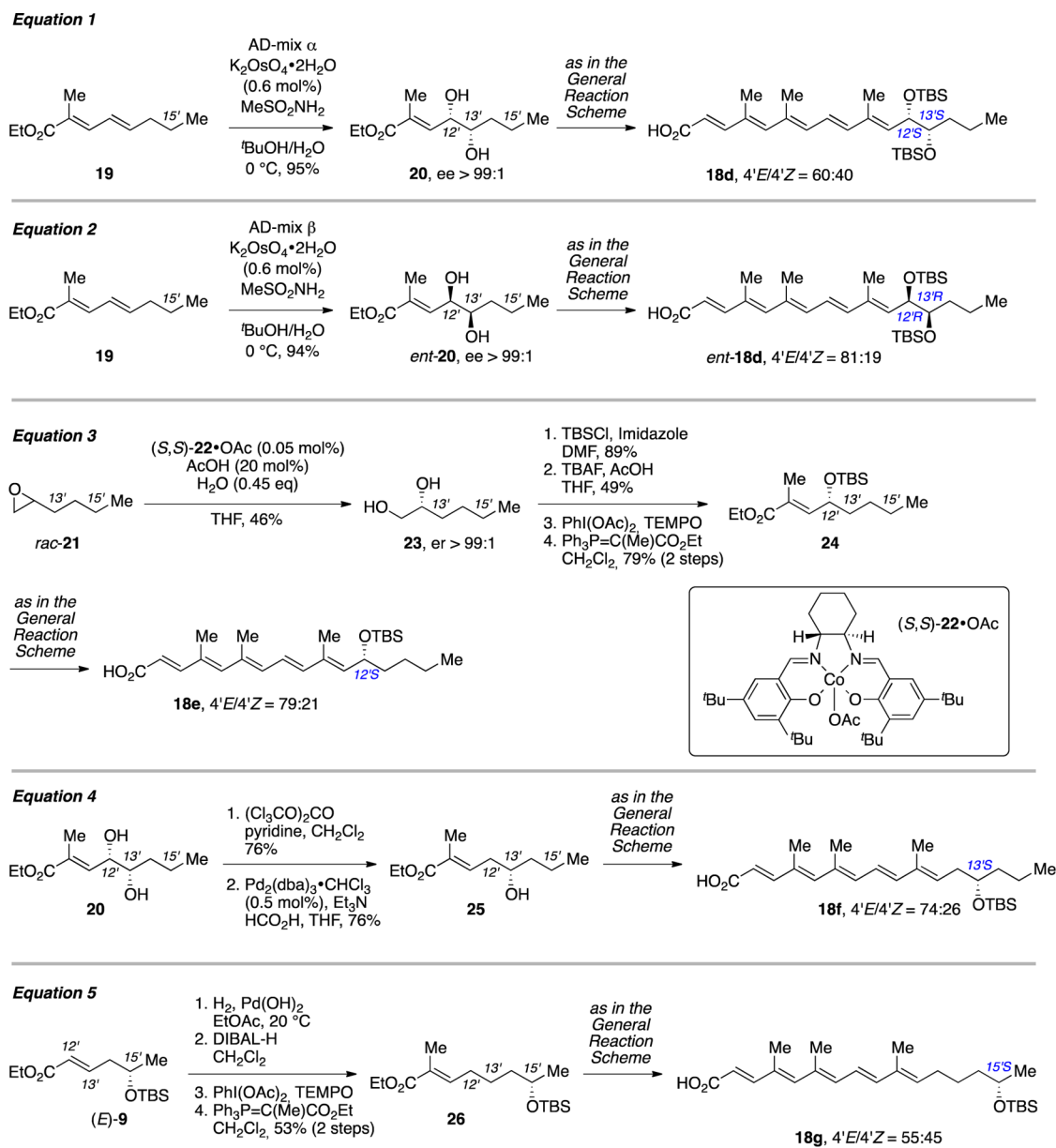
stimulation of N-WASP resulted in loss of adhesion and eventually cell death by anoikis. In vivo, injection of mycolactone into the ears of mice altered the adhesion of keratinocytes, leading to the rupture of the epidermis. Mycolactone-induced defects in cell adhesion and skin ulceration were efficiently suppressed by the N-WASP inhibitor wiskostatin, demonstrating the critical role of N-WASP in these processes.

In addition to killing anchorage-dependent cells, mycolactone inhibits at noncytotoxic doses the capacity of immune cells to express membrane and secreted proteins.^{16–23} Intriguingly, this function was efficiently blocked by wiskostatin,²¹ suggesting that Arp2/3-mediated polymerization of actin is involved, but wiskostatin was ineffective at rescuing cytokine production by mycolactone-treated macrophages. Further work

will be needed to determine if WASP/N-WASP or a distinct molecular receptor mediates the immunomodulatory properties of mycolactone. Finally, mycolactone was recently reported to stimulate angiotensin II receptor (AT2R) pathways in neurons.²⁴ It will be interesting to determine if this new feature of mycolactone relates to the activation of neural (N) WASP and resists the inhibitory effect of mycolactone on membrane protein expression.²⁵

The chemical synthesis of natural products and their derivatives allows the biological exploration of complex systems, and programs centered on the synthesis and structural modulation of mycolactone A/B have been reported by Kishi, Altmann, and us (Figure 2).² Kishi clearly opened the way to chemical modifications of this exotoxin with several generations of elegant total syntheses of mycolactone A/B and also of the

Scheme 2. Synthesis of Monodeoxy and Dideoxy Southern Fragments of Mycolactone Analogues



comprises two C14–C20 truncated analogues in which the C5-hydroxy group is either free (**5a**) or esterified with the natural C1'–C16' southern fragment of mycolactone A/B (**5b**). The third class includes a single ester of the polyenic fragment (**6a**), whereas the fourth class encompasses the fluorescent derivative **7** used for in vitro imaging. We demonstrated that the less potent derivatives were **5a** and **6a** and that suppression of the southern (**4a**) or northern fragment (**5b**) of C8-desmethyl mycolactone A/B led to a significant drop in cytopathic activity. The importance of the absolute configurations of the C12',C13',C15'-stereocenter (mycolactone numbering) was also stressed out, since the more potent analogues possessed the natural (12'S,13'S) configurations (as in **4b**) whereas the C15'-configuration was shown to be less crucial. In line with the known cytopathic activity of mycolactone C (the C12'-deoxy mycolactone A/B, LC₅₀ = 186 nM),^{2,30} analogue **4e** led to 49% of cell rounding at 10 μM. Further studies on the more potent analogue **4b** uncovered that the lowest concentration inducing 90% of cell rounding was 5 μM, to be compared with

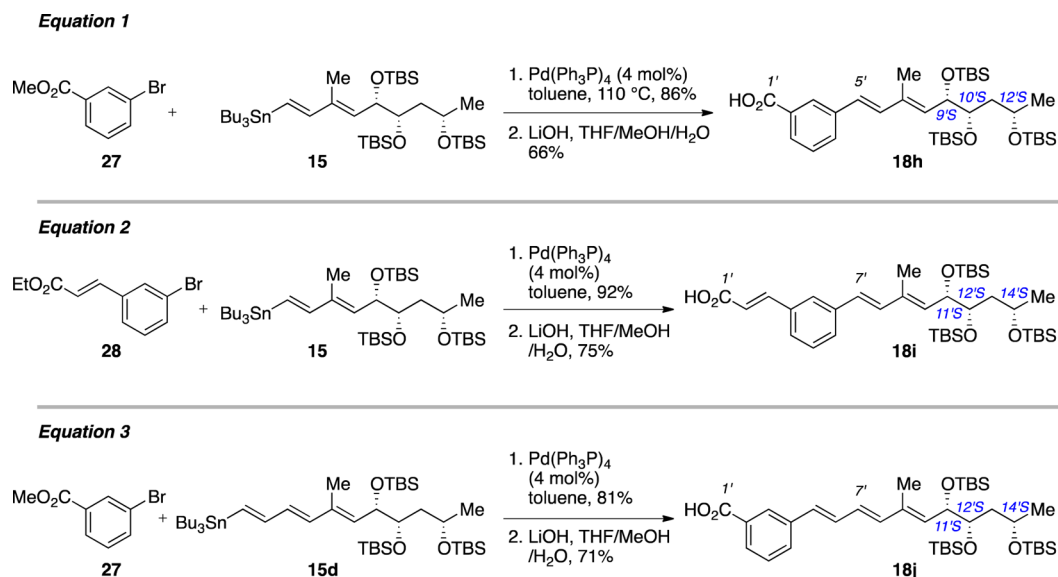
the 40 nM found in our laboratory for the natural mycolactone A/B. Consistent with the different activities reported for the nine naturally occurring mycolactones (that differ only by the structure of this southern fragment),² this first set of data clearly pointed toward the importance of the C1'–C16' southern fragment for biological activity.

To gain further insight into structure–activity relationships, we synthesized novel analogues of mycolactone including additional variations in the southern chain and examined their individual capacity to bind WASP and N-WASP in vitro. We conclude that mycolactone binds and destabilizes the auto-inhibited fold of WASP and N-WASP primarily via its lactone core and southern chain.

RESULTS AND DISCUSSION

We first focused on the southern fragment and introduced systematic variations in the C12',C13',C15'-stereocenter (both from a substitution and configuration point of view) as well as aromatic moieties in the polyenic motif.

Scheme 3. Inclusion of Aromatic Moieties in the Southern Fragment of Mycolactone Analogues



Variation of the C12',C13',C15'-Stereocluster. The C12',C13',C15'-stereocluster is a crucial region of mycolactones, as shown in an early study by Small⁷ and more recently by Altmann and Pluschke³¹ and us.³³ Besides the synthesis of the *syn-syn* cluster present in the natural product, an efficient access to all possible isomers has important implications in terms of SAR studies. We specifically targeted the *anti-syn* (**18a** and *ent-18a*), *anti-anti* (**18b** and *ent-18b*), and *syn-anti* (**18c**) C12',C13',C15'-stereotriads using a catalytic asymmetric approach to set up the three stereocenters (Scheme 1, General Reaction Scheme). Starting from β -silyloxyaldehyde **8**, (*Z*)- α,β -unsaturated ester **9** was obtained as a single isomer because of an Ando olefination reaction.^{35,36} Dihydroxylation³⁷ of the latter using commercially available AD-mix α led to compound **10a** in a 90:10 diastereomeric ratio, in which the C12',C13'-stereocenters (mycolactone numbering) possessed the *anti* relative configuration. Further chain elongation delivered the (*E,E*)-dienylstannane **15a** which is then cross-coupled with iodotrienoate **16** using Liebeskind's copper(I) thiophenecarboxylate^{38–40} as a mediator, at room temperature in NMP, following our first generation synthesis.³³ Although the yield over two steps is moderate, this cross-coupling features an active, stable, and economic mediator. A last saponification finally delivered the desired C1'-C16' southern fragment *anti-syn* **18a**. The same synthetic strategy was used for the preparation of *anti-anti* **18b** (with AD-mix β) and *syn-anti* **18c** (Scheme 1, eq 1), switching the Ando olefination for a classical Horner–Wadsworth–Emmons reaction. Eventually, starting from β -silyloxyester *ent-9*, the last two complementary southern fragments *anti-anti-ent-18b* and *anti-syn-ent-18a* were obtained (Scheme 1, eq 2).

On the basis of the structure of mycolactone **C**,^{2,30} it was relevant to investigate structural modulation of the southern fragment in the deoxy series. In addition to our previous analogue **4e**, two new derivatives were specifically targeted, **18d** and *ent-18d*, featuring a deoxy-C15' position (Scheme 2, eqs 1 and 2). An asymmetric dihydroxylation of the more electron rich double bond of the dienolate (*E,E*)-**19** using both pseudo-enantiomers of AD-mix led to the C15'-deoxy fragment **20** and *ent-20* as single enantiomers. The enantiomeric excess and absolute configuration of **20** were proven by conversion to the

bis-methoxyphenyl esters according to the method of Riguera.^{41–43} Following the previous route, ester **20** was converted to the desired C15'-deoxy southern fragment **18d**. On the other hand, *ent-20* was transformed to the desired carboxylic acid *ent-18d*.

Finally, the excision of two hydroxyl groups from the southern fragment was studied (Scheme 2, eqs 3–5). Several synthetic routes leading to dideoxy-C13',C15' **18e** were evaluated, and only a Jacobsen hydrolytic kinetic resolution^{44,45} (HKR) of commercially available epoxide *rac-21* proved successful (Scheme 2, eq 3). By use of a catalytic amount of **22** (0.05 mol %), this HKR delivered on a multigram scale diol **23** in excellent yield and enantiomeric excess. Conversion of the latter to α,β -unsaturated ester **24** and further to the desired dideoxy-C13',C15' fragment **18e** proceeded smoothly.

Finally, the last two dideoxy fragments **18f** and **18g** were prepared in several steps starting from previous reaction intermediates, diol **20** and α,β -unsaturated ester (*E*)-**9**, respectively (Scheme 2, eqs 4 and 5). It should be noted that all the southern fragments **18** are synthesized as a dynamic mixture of C4'-C5' isomers.⁴⁶

Inclusion of Aromatic Moieties in the Southern Fragment. As evocated in the previous section, the southern fragment of the natural toxin exists as a dynamic mixture of C4'-C5' isomers, the *Z*-isomer being predominant because of allylic strain between the C4'- and C6'-methyl groups in the corresponding *E*-isomer.² From a structure–activity relationship point of view, a series of analogues deprived of this allylic strain would be of interest by giving insights in the biological activities of stereodefined isomers of the pentaenic fragment. We thus embarked in the synthesis of three southern fragments (Scheme 3, **18h–j**) in which an aromatic motif would replace a portion of the polyenic fragment. Three structural modulations were targeted with the replacement of the C1'–C7' fragment with a benzoic (**18h**) or a cinnamic acid (**18i**) and the replacement of the C1'–C4' fragment with a benzoic acid (**18j**). The syntheses relied on the Stille cross-coupling reactions of aryl bromides **27** and **28** with the appropriate vinylstannanes followed by ester hydrolysis (Scheme 3, eqs 1–3).

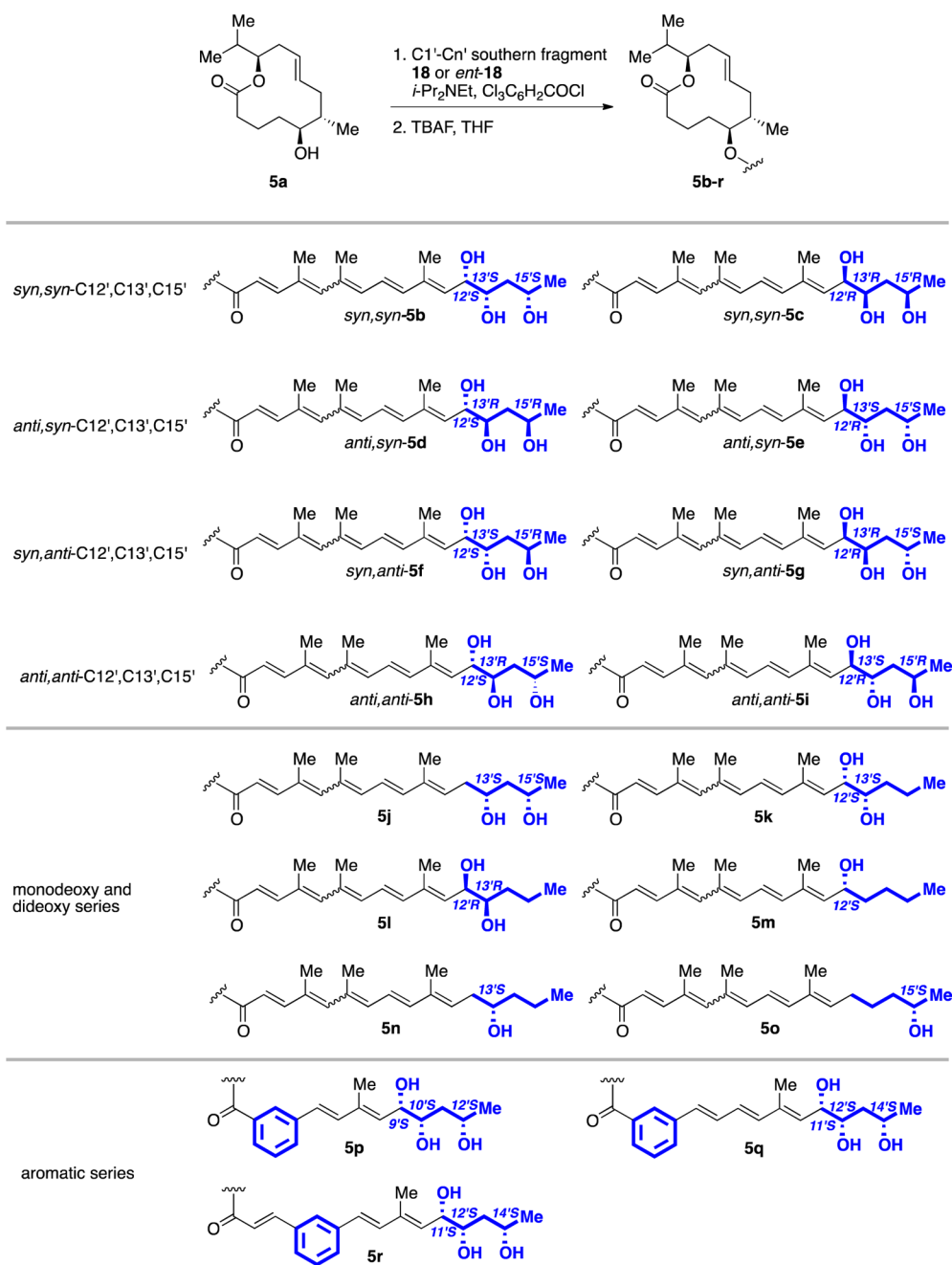


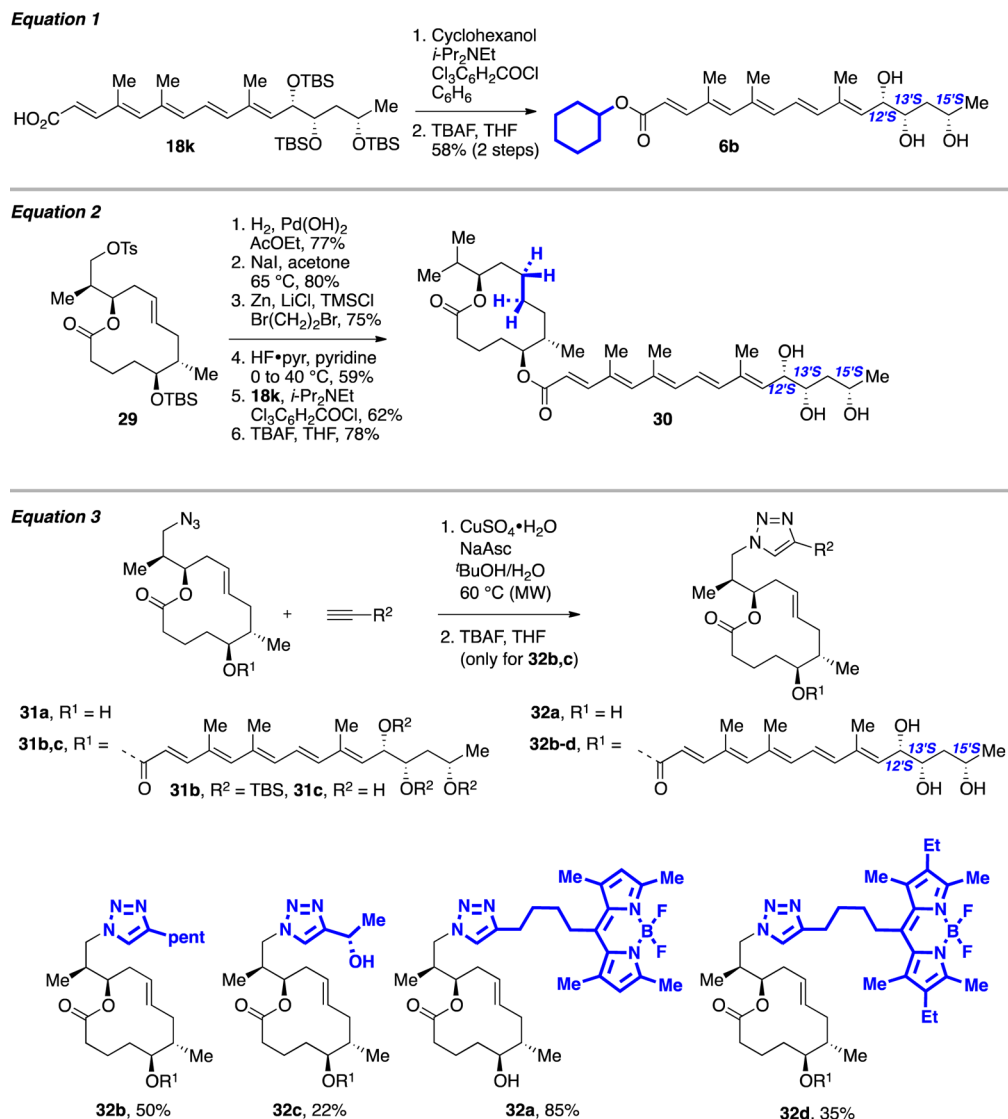
Figure 3. Synthesis of analogues 5b–r via esterification of 5a with southern fragments 18 and *ent*-18.

Final Crafting of the Mycolactone Analogues. Having in hand a set of 13 new C1'–C16' southern fragments, we next turn our attention to their esterification with a simplified core structure of mycolactone. As shown in Figure 3, Yamaguchi conditions followed by global deprotection with tetrabutylammonium fluoride delivered the desired new variants 5c–r.

Simplification of the Core Structure and Inclusion of Fluorescent Motifs. Another set of two analogues (6b and 30) was obtained by esterification of 18k, the natural southern fragment of mycolactone A/B (protected as a tri-TBS ether at C12', C13', and C15'), with cyclohexanol (Scheme 4, eq 1) and with the saturated mycolactone core, obtained in four steps from the first generation synthesis intermediate 29 (Scheme 4, eq 2).

The fluorescent analogue of mycolactone 7 (Figure 2) was helpful in previous studies to assess the colocalization of mycolactone with WASP in T lymphocytes.¹⁴ On the basis of the known first generation intermediates 31a and 31b, five C13-triazolomycolactone analogues were prepared by [3 + 2] cycloadditions with the appropriate alkynes in moderate to good yields (Scheme 4, eq 3), leading to the generation of novel fluorescent derivatives (32a and 32d). The red-fluorescing 32d may provide a useful alternative to green-fluorescing 7 in multicolor imaging studies. Since 32a only differs from 7 by the absence of the southern fragment, it represents a valuable tool to investigate the role of this chain in mycolactone diffusion in vivo. As shown in Figure 4, 32a and 7 both penetrated epithelial cells with saturable kinetics, reaching a plateau after 24 h of incubation. Consistent with passive

Scheme 4. Simplification of the Core Structure and Inclusion of Fluorescent Motifs



diffusion,⁴⁷ the time-dependent accumulation of **32a** in the cell cytoplasm was faster than that of **7**.

Mycolactone Analogues Bind to WASP and N-WASP.

As previously described, binding of natural mycolactone A/B to the 502 amino acids protein WASP involves a minimal linear domain of 114 amino acids (200–313) and binding to N-WASP involves at least 91 amino acids (186–276) out of the 505 of the protein.¹⁴ Two interaction sites have been found, the first one downstream of the CRIB region (Cdc42/Rac-interactive-binding, 14 amino acids in WASP and N-WASP (238–251 and 203–216, respectively)) and the second one in the basic region (lysine-rich portion, 12 and 15 amino acids in WASP and N-WASP, respectively (224–235 and 186–200)). The binding of all mycolactone analogues to WASP and N-WASP was assessed through their capacity to displace C12'-biotinylated mycolactone A/B (the synthesis of which was reported previously)¹⁴ from the mycolactone binding domains (MBD) of WASP or N-WASP in ELISA.

The results obtained with the WASP MBD are shown in Figures 5 and 6, as expressed by the half maximal inhibitory concentrations relative to natural mycolactone A/B, which displayed an IC₅₀ of 32.3 ± 22.1 μM (Figure 6). Comparable

results were obtained with N-WASP (data not shown). No binding could be detected with the **5a** and **4a** analogues, which correspond to the simplified core structure of mycolactone A/B bound or not to the northern chain (Figure 5A). In striking contrast, mycolactone core linked to southern chain (**5b**) bound WASP comparably to mycolactone (IC₅₀ = 21.5 ± 0.7 μM, Figure 6). In comparison, a cyclohexyl ester of the southern fragment of mycolactone A/B (**6b**) was far less reactive (IC₅₀ = 135 ± 21.2 μM).

We have previously shown that removal of the C8-methyl group of mycolactone A/B, as in **4b**, led to a 125-fold decrease in cytopathic activity compared to the natural toxin.³³ The present results demonstrate that **4b** is only 3-fold less efficient for the binding to WASP, with an IC₅₀ of 97.5 ± 7.1 μM vs 32.3 ± 22.1 μM for natural mycolactone A/B (Figure 5B and Figure 6). Compared to **5b** (IC₅₀ = 21.5 ± 0.7 μM), addition of a (triazol-4-yl)ethanol to the core in northern position (**32c**) limited binding (IC₅₀ = 170 μM), as did the selective epimerization of C12' and C15' (**5i**, IC₅₀ = 100 μM) or the removal of two hydroxyl groups of the southern fragment (C13',C15'-dideoxy **5m**, IC₅₀ = 350 ± 70.7 μM) or one hydroxyl group in C15' (**5k**, IC₅₀ = 250 ± 0.7 μM). Saturation

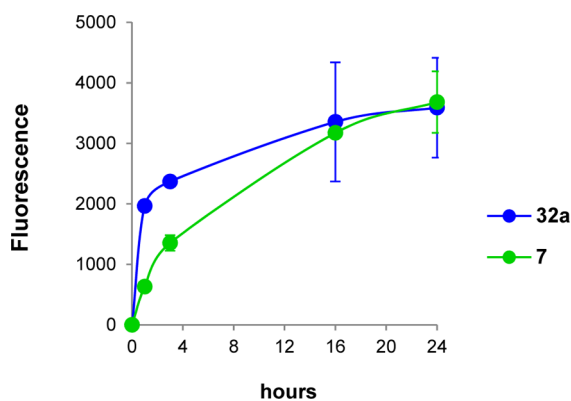


Figure 4. Diffusion of fluorescent mycolactone derivatives into epithelial cells. The kinetics of intracellular accumulation of **32a** and **7** in HeLa cells are shown. HeLa cells were seeded in 96-well plates (10^4 cells/well) and incubated at 37°C for 24 h prior to the addition of fluorescent derivatives or vehicle as control. Cells were rinsed three times with phosphate buffered saline (PBS) before reading of the fluorescence on a microplate reader. Data are mean intensities of fluorescence of treated cells per well ($\lambda_{\text{excitation}} = 490\text{ nm}$; $\lambda_{\text{emission}} = 520\text{ nm}$) relative to controls, as measured in duplicate. They are representative of two independent experiments.

of the C8–C9 π -system (**30**) or introduction of a meta-disubstituted aromatic motif on the C1'-carbonyl (**5p**, **5q**) was less detrimental to binding, with IC_{50} in the 60–70 μM range (Figure 5). Notably, 14 other analogues demonstrated an efficient binding to the MBD of WASP, with IC_{50} in the 10–44 μM range (Figure 6). These included the (hetero)aromatic derivatives **32b** ($35 \pm 7.1\ \mu\text{M}$) and **5r** ($35 \pm 7.1\ \mu\text{M}$), the C12',C15'-dideoxy **5n** ($23\ \mu\text{M}$), the C12'-deoxy **5j** ($28 \pm 5.7\ \mu\text{M}$), and the C15'-deoxy **5l** ($27 \pm 1.4\ \mu\text{M}$). When the three hydroxyl groups were present in C12', C13', and C15' (**5b–h**), IC_{50} values comparable to that of mycolactone A/B were observed.

Overall, these investigations demonstrated that (1) an efficient binding to the MBD of WASP was observed even with mycolactone analogues lacking the northern fragment and the C8-methyl group, one of the best representative example being **5b**, which is as potent as natural mycolactone; (2) the relative and absolute configurations of the C12', C13', and C15' stereocenters can be modified individually without any impact on the binding, as in **5c–h**; (3) when two stereocenters are inverted simultaneously, a sharp decrease in binding is only observed for **5i** ($100\ \mu\text{M}$) which corresponds to the inversion of the C12',C15' stereocenters; (4) one or two hydroxyl groups can be selectively excised at the C12', C13', and/or at the C15' positions (except for compounds **5k,m,i**); (5) eventually, an alkyl-substituted triazole is tolerated in the northern fragment (**32b**) and an aromatic ring can be embedded in the southern fragment when connected to the C3' position (**5r**).

5b Mimics Mycolactone for WASP Activation and Alteration of Cell Adhesion. Having demonstrated that mycolactone activates WASP by destabilizing the autoinhibited fold of the protein,¹⁴ we examined the impact of the closest structural analogue of the natural toxin, **5b**, on the maintenance of intramolecular interactions. A glutathione *S*-transferase (GST) fused version of the MBD in WASP was immobilized on glutathione beads and used to capture WASP VCA in solution (Figure 7A). The resulting complex was incubated with **5b** and dissociation monitored by electrophoretic analysis of pulled down products. Strikingly, **5b** mimicked mycolactone

in the induction of a dose-dependent release of VCA from immobilized MBD.¹⁴ Similar results were obtained with the MBD in N-WASP (data not shown).

Since mycolactone-mediated activation of N-WASP causes the detachment-induced death of epithelial cells,¹⁴ we then compared mycolactone and **5b** for capacity to inhibit cell adhesion. We used the xCELLigence System (Roche Applied Science), as it allows the dynamic monitoring of cell adhesion through the measurement of electrical impedance across interdigitated microelectrodes integrated on the bottom of tissue culture E-Plates. Like mycolactone, **5b** reduced the adhesion capacity of HeLa cells (Figure 7B). In contrast, the mycolactone analogue **5a**, which is unable to bind WASP, did not alter cell adhesion at the same concentration (data not shown). Of note, **5b** induced cell retraction at concentrations >300 times higher than those of mycolactone (8 μM vs 26 nM), suggesting that the synthetic compound is less able to gain access to N-WASP in the intracellular environment.

CONCLUSION

In the present study, we report the synthesis of 23 new analogues of mycolactone A/B together with their capacity to bind WASP/N-WASP. A subset of 14 simplified analogues missing the northern polyketide chain demonstrated a binding potency equivalent to that of the natural toxin. Notably, the one bearing mycolactone A/B southern chain also showed capacity to activate WASP/N-WASP in vitro and induced cytopathic effects. In addition to identification of the structural basis of cytotoxicity in mycolactone, our study thus paves the way for mechanistic studies of the mycolactone/WASP complex using a simplified analogue as a surrogate of the natural exotoxin.

Unraveling the role of WASP/N-WASP in mycolactone-induced immune suppression not only will help better understand the pathogenesis of BU disease but also will advance our understanding of the dialogue between the cytoskeleton of immune cells and their effector functions. Resolving the structure of the mycolactone/WASP complex should generate insights into the physical mechanism of WASP activation by mycolactone. It may help identify domains of N-WASP/WASP that bind mycolactone without interfering with the function of endogenous proteins, of interest to neutralize the activity of this major virulence factor of *M. ulcerans*.

EXPERIMENTAL SECTION

General Procedures. NMR spectra were recorded on Bruker AV 300 or AV 400 spectrometer and calibrated using undeuterated solvent as internal reference, unless otherwise indicated. Coupling constants (J) were reported in hertz. Attached proton tests (APT) were performed to distinguish between different carbons in the ^{13}C NMR spectra. The following abbreviations were used to explain multiplicities: s = singlet, d = doublet, t = triplet, q = quartet, m = multiplet, and b = broad. Optical rotations were recorded on a PerkinElmer polarimeter (model 341LC) and are expressed in $\text{deg}\cdot\text{cm}^2\cdot\text{g}^{-1}$ units. High-resolution mass spectra were recorded on an Agilent Q-TOF (ESI) coupled with an Agilent 1100 series HPLC instrument. All reactions were carried out in oven-dried glassware under an argon atmosphere using dry solvents, unless otherwise noted. Tetrahydrofuran (THF) was distilled under argon from sodium benzophenone. Toluene was dried using the Dry Solvent Station GT S100 developed by Glass Technology, and dichloromethane was distilled over CaH_2 . All other anhydrous solvents were purchased from Sigma-Aldrich. Reagents were purchased from Aldrich, Acros, or Alfa Aesar and used without further purification, unless otherwise noted. Yields refer to chromatographically and spectroscopically (^1H NMR) homogeneous materials, unless otherwise noted. Reactions were monitored by thin-

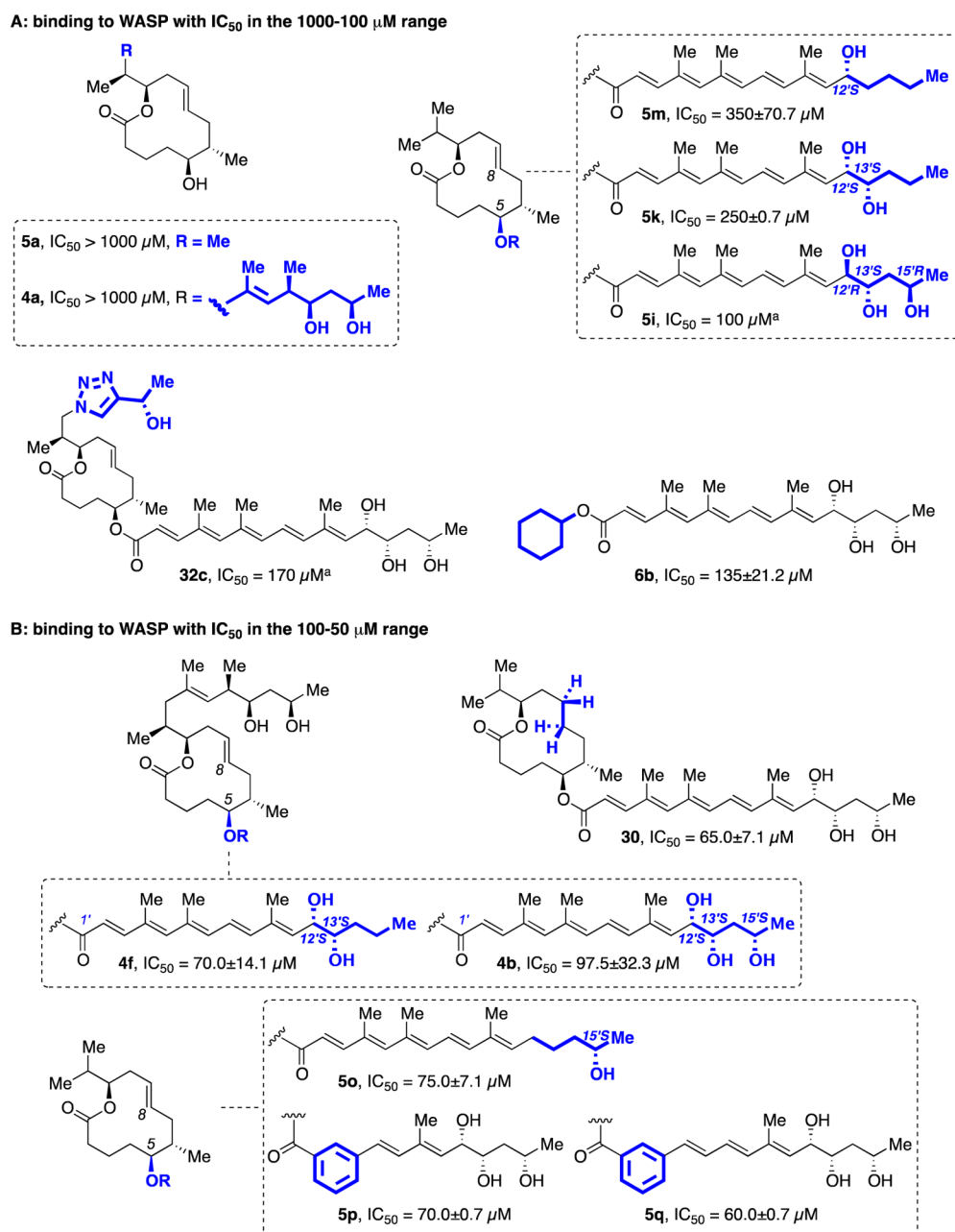


Figure 5. Mycolactone analogues binding WASP with IC₅₀ in the 1000–50 μM range. Data are mean IC₅₀ ± SD relative to vehicle controls, as measured in replicate ($n \geq 2$). Footnote letter in the figure indicates the following: ^aSingle determination.

layer chromatography (TLC) carried out on Merck TLC silica gel 60 F254 glass-coated plates, using UV light, iodine vapor, potassium permanganate as visualizing agents. All separations were performed by flash chromatography on Merck silica gel 60 (40–63 μm) unless otherwise specified. All compounds used in biological assays were analyzed by ¹H and ¹³C NMR and conformed to purities of ≥95%.

(*S,Z*)-Ethyl 5-((*tert*-Butyldimethylsilyloxy)hex-2-enoate (Z)-9). To a stirred solution of (*o*-Tol)₂P(O)CH₂CO₂Et^{35,36} (4.70 g, 13.50 mmol, 1.3 equiv) in dry THF (105 mL), under a nitrogen atmosphere, was added NaI (1.56 g, 10.40 mmol) at 0 °C. After 5 min, NaH (60% dispersion, 540 mg, 13.50 mmol, 1.3 equiv) was added. The resulting solution was cooled to –78 °C, and **8**¹⁰ (2.10 g, 10.40 mmol) was added dropwise. After stirring 3 h at –78 °C, a saturated aqueous NH₄Cl solution was added and the reaction mixture was extracted three times with Et₂O. The combined organic extracts were washed with brine, dried over MgSO₄, filtered, and concentrated under reduced pressure. The crude product was purified by flash chromatography (cyclohexane/EtOAc 9:1) to afford (Z)-9 (2.11 g,

7.75 mmol, 75%) as a pale yellow oil. ¹H NMR (CDCl₃, 300 MHz) δ 6.35 (dt, $J = 11.6, 6.3$ Hz, 1H), 5.84 (dt, $J = 11.6, 1.7$ Hz, 1H), 4.17 (q, $J = 7.1$ Hz, 2H), 3.96 (dq, $J = 6.6, 6.1, 5.0$ Hz, 1H), 2.88–5.68 (2H), 1.29 (t, $J = 7.1$ Hz, 3H), 1.16 (d, $J = 6.1$ Hz, 3H), 0.88 (s, 9H), 0.06 (s, 3H), 0.05 (s, 3H). ¹³C NMR (CDCl₃, 100 MHz) δ 166.4, 146.9, 120.7, 67.9, 59.8, 38.6, 25.8 (3C), 23.7, 18.0, 14.2, –4.5, –4.8. HRMS-ESI calculated for C₁₄H₂₉O₃Si: m/z 273.1886 ([M + H]⁺). Found: m/z 273.1881 ([M + H]⁺). [α]_D²⁰ +12.9 (c 1.4, CHCl₃).

(2*S,3S,5S*)-Ethyl 5-((*tert*-Butyldimethylsilyloxy)-2,3-dihydroxyhexanoate (10a). To a stirred solution of AD-mix α (5.06 g, 0.4% osmium, 1% (DHQ)₂PHAL) in a mixture 1:1 *t*-BuOH/H₂O (30:30 mL) were added successively methanesulfonamide (300 mg, 3.15 mmol 0.9 equiv), potassium osmate(VI) dihydrate (10 mg, 27.14 μmol, 0.6 mol %), and (DHQ)₂PHAL (114 mg, 0.15 mmol, 4 mol %). The mixture was stirred at room temperature until two clear phases were produced. The solution was cooled to 0 °C, whereupon the inorganic salts partially precipitate, and (Z)-9 (1.00 g, 3.68 mmol) was then added. After stirring 48 h at 0 °C, Na₂SO₃ (9.2 g) was added

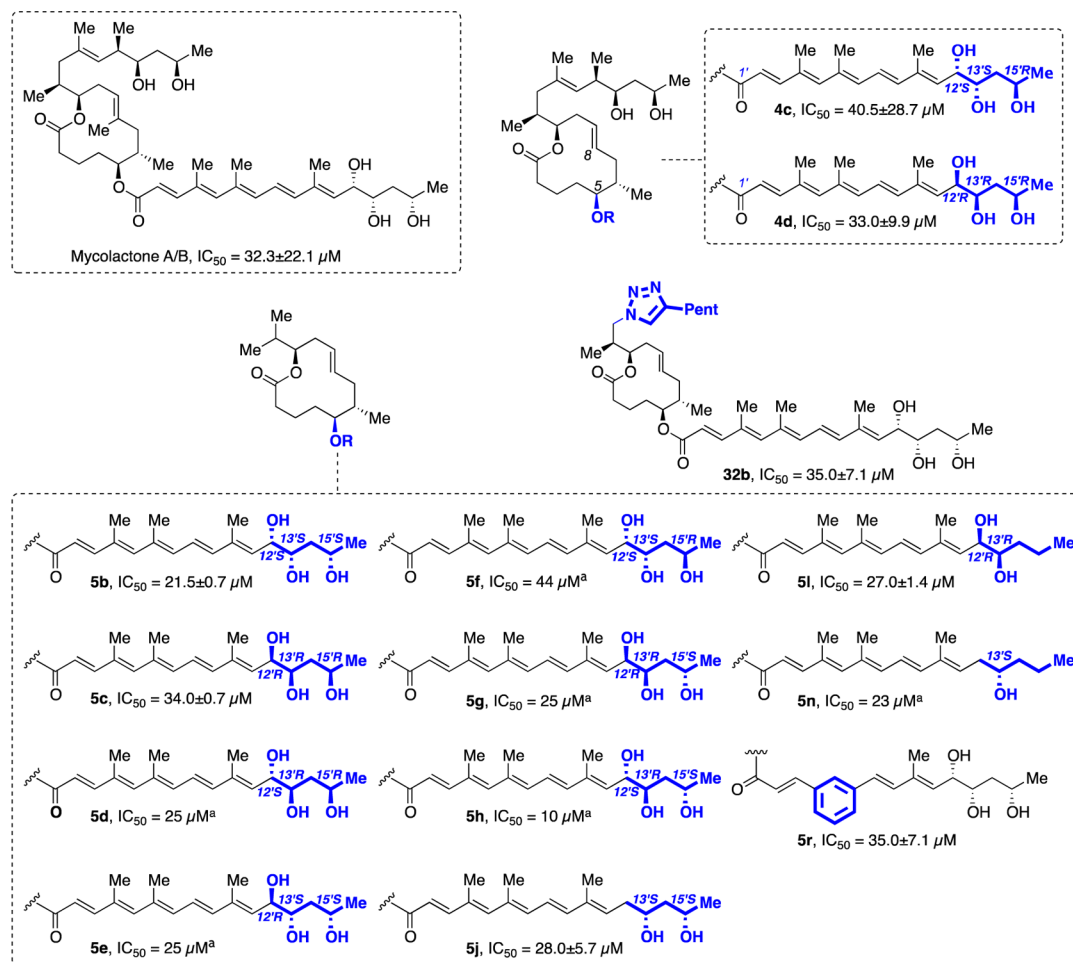
Binding to WASP with IC₅₀ in the 50–10 μM range

Figure 6. Mycolactone analogues binding WASP with IC₅₀ in the 50–10 μM range. Data are mean IC₅₀ ± SD relative to vehicle controls, as measured in replicate ($n \geq 2$). Footnote letter in the figure indicates the following: ^aSingle determination.

and the reaction mixture was stirred for 30 min at room temperature. The mixture was extracted three times with EtOAc. The combined organic extracts were washed with an aqueous KOH solution (2 M), brine, dried over MgSO₄, filtered, and concentrated under reduced pressure. The crude product was purified by chromatography (cyclohexane/EtOAc 8:2) to give an inseparable mixture of diastereoisomers (700 mg, 2.29 mmol, 62%, 90:10 in favor of the desired diastereoisomer **10a**) as a colorless oil. ¹H NMR (CDCl₃, 300 MHz) δ 4.34–4.18 (5H), 3.29 (br s, 1H), 3.00 (br s, 1H), 1.80 (m, 1H), 1.40 (m, 1H), 1.32 (t, $J = 7.1$ Hz, 3H), 1.22 (d, $J = 6.2$ Hz, 3H), 0.89 (s, 9H), 0.10 (s, 3H), 0.09 (s, 3H). ¹³C NMR (CDCl₃, 100 MHz) δ 172.6, 74.3, 70.1, 66.5, 61.8, 39.3, 25.8 (3C), 23.1, 17.9, 14.2, –4.5, –5.1. HRMS-ESI calculated for C₁₄H₃₁O₅Si: m/z 307.1941 ([M + H]⁺). Found: m/z 307.1940 ([M + H]⁺).

(2*R*,3*S*,5*S*)-2,3,5-Tris(*tert*-butyldimethylsilyloxy)hexan-1-ol (11). To a stirred solution of **10a** (700 mg, 2.29 mmol) in dry DMF (23 mL), under a nitrogen atmosphere, were added *tert*-butyldimethylsilyl chloride (2.07 g, 13.70 mmol, 6 equiv), imidazole (622 mg, 9.15 mmol, 4 equiv), and DMAP (56 mg, 0.46 mmol, 0.2 equiv). The reaction mixture was stirred at room temperature for 48 h. The resulting solution was hydrolyzed with water, and the aqueous layer was extracted three times with a mixture of cyclohexane and DCM (9:1). The combined organic extracts were washed with water, brine, dried over MgSO₄, filtered, and concentrated under reduced pressure. The crude product was purified by chromatography (cyclohexane/EtOAc 20:1) to give an inseparable mixture of diastereoisomeric esters (766 mg, 1.43 mmol, 63%, 90:10 diastereomeric ratio) as a colorless oil. ¹H NMR (CDCl₃, 300 MHz) δ 4.15 (q, $J = 7.1$ Hz, 2H), 4.15 (d, $J = 2.3$ Hz, 1H), 4.07 (ddd, $J = 7.5, 4.3, 2.3$ Hz, 1H), 3.89 (m, 1H), 1.79 (ddd, $J = 14.1, 7.8, 4.1$ Hz, 1H), 1.59 (ddd, $J = 14.1, 7.6, 4.6$ Hz, 1H), 1.28 (t, $J = 7.1$ Hz, 3H), 1.16 (d, $J = 6.1$ Hz, 3H), 0.92 (s, 9H), 0.88 (s, 9H), 0.87 (s, 9H), 0.11 (s, 3H), 0.09 (s, 3H), 0.08 (s, 3H), 0.07 (s, 3H), 0.06 (s, 3H), 0.05 (s, 3H). ¹³C NMR (CDCl₃, 100 MHz) δ 171.7, 77.5, 73.3, 65.8, 60.5, 44.6, 25.93 (3C), 25.90 (3C), 25.8 (3C), 24.6, 18.4, 18.1, 18.0, 14.2, –3.5, –4.0, –4.3, –4.6, –4.9, –5.3. HRMS-ESI calculated for C₂₆H₅₈O₅NaSi₃: m/z 557.3490 ([M + Na]⁺). Found: m/z 557.3492 ([M + Na]⁺).

To a stirred solution of the latter compound (766 mg, 1.43 mmol) in dry DCM (12 mL), under a nitrogen atmosphere, was added DIBAL-H (2.2 mL, 1.5 M in toluene, 3.15 mmol, 2.2 equiv) at 0 °C. The reaction mixture was stirred at 0 °C for 1 h. Saturated aqueous Rochelle salt solution was then added, and the resulting mixture was warmed to room temperature and vigorously stirred overnight. The aqueous layer was extracted with Et₂O, and the combined organic extracts were washed with water, brine, dried over MgSO₄, filtered, and concentrated under reduced pressure. The crude alcohol was purified by chromatography (cyclohexane/EtOAc 95:5) to afford **11** (511 mg, 1.04 mmol, 73%) as the major diastereoisomer and **11b** as the minor one (51 mg, 0.10 mmol, 7%). ¹H NMR (CDCl₃, 300 MHz) δ 3.97–3.90 (2H), 3.73 (dd, $J = 12.5, 6.6$ Hz, 1H), 3.63–3.57 (2H), 1.69 (ddd, $J = 14.2, 8.3, 3.8$ Hz, 1H), 1.50 (ddd, $J = 14.2, 7.5, 3.6$ Hz, 1H), 1.17 (d, $J = 6.2$ Hz, 3H), 0.92 (s, 9H), 0.89 (s, 9H), 0.88 (s, 9H), 0.13 (s, 3H), 0.11 (s, 3H), 0.10 (s, 3H), 0.10 (s, 3H), 0.08 (s, 6H). ¹³C NMR (CDCl₃, 100 MHz) δ 76.4, 73.6, 66.2, 63.7, 45.5, 26.0 (3C), 25.94 (3C), 25.93 (3C), 24.9, 18.3, 18.2, 18.0, –3.4, –3.9, –4.2, –4.3, –4.5, –4.6. HRMS-ESI calculated for C₂₄H₅₇O₄Si₃: m/z 493.3565 ([M

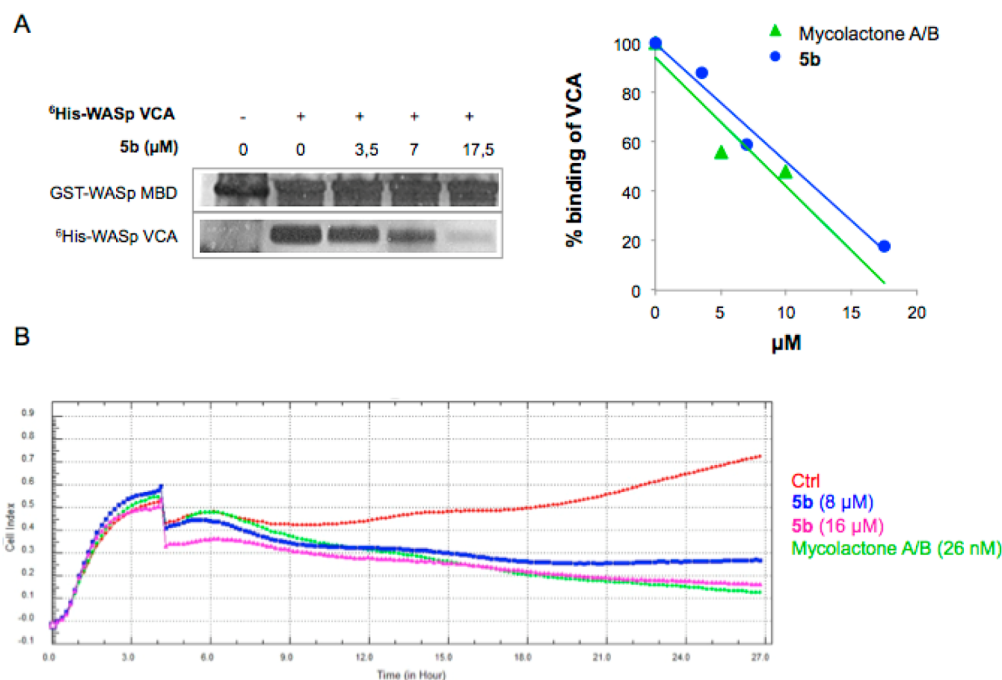


Figure 7. Effects of **5b** on WASP activation and epithelial cell adhesion. (A) Dose-dependent displacement of WASP MBD-bound VCA by **5b**: silver staining of WASP MBD and VCA, after incubation of GST-fused WASP MBD (immobilized on glutathione-sepharose beads) with VCA in the presence of increasing amounts of **5b**, and analysis of bead-bound products by gel electrophoresis (left). The percentage of binding of VCA (right) is calculated as a function of the concentration of mycolactone A/B and **5b**, relative to controls. (B) Reduction of epithelial cell adhesion upon addition of **5b**. HeLa cells were left to adhere for 4 h at 37 °C prior to the addition of mycolactone A/B (26 nM), **5b** (8 and 16 μM), or DMSO as vehicle control (Ctrl) and monitoring of impedance for 24 h. Data are mean cell index, calculated in quadruplicate.

+ H⁺). Found: m/z 493.3561 ([M + H]⁺). [α]_D²⁰ +9.7 (c 0.9, CHCl₃).

(2S,3S,5S)-2,3,5-Tris((tert-butylidimethylsilyloxy)hexanal (12). To a stirred solution of **11** (500 mg, 1.01 mmol) in dry DCM (2.0 mL), under a nitrogen atmosphere, were added iodosobenzene diacetate (360 mg, 1.12 mmol, 1.1 equiv) and TEMPO (16 mg, 0.10 mmol, 0.1 equiv) at 0 °C. The reaction mixture was stirred at room temperature for 5 h. Water was then added to the reaction mixture which was extracted three times with DCM. The combined organic extracts were washed with water, brine, dried over MgSO₄, filtered, and concentrated under reduced pressure. The crude aldehyde **12** was used in the next step without further purification. ¹H NMR (CDCl₃, 300 MHz) δ 9.62 (d, J = 1.9 Hz, 1H), 4.08 (m, 1H), 3.91 (ddd, J = 7.9, 6.1, 4.2 Hz, 1H), 3.87 (dd apt, J = 2.0 Hz, 1H), 1.75 (ddd, J = 14.1, 7.9, 4.3 Hz, 1H), 1.61 (ddd, J = 14.1, 7.2, 4.2 Hz, 1H), 1.17 (d, J = 6.1 Hz, 3H), 0.94 (s, 9H), 0.89 (s, 9H), 0.87 (s, 9H), 0.13 (s, 3H), 0.11 (s, 6H), 0.08 (s, 9H).

(4R,5S,7S,E)-Ethyl 4,5,7-Tris((tert-butylidimethylsilyloxy)-2-methyloct-2-enoate (13). To a stirred solution of crude aldehyde **12** in 1,2-dichloroethane (5 mL), under a nitrogen atmosphere, was added (1-ethoxycarbonyl ethylidene)triphenylphosphorane (550 mg, 1.50 mmol, 1.5 equiv) at room temperature. The reaction mixture was warmed to 70 °C and stirred for 48 h. The resulting solution was then cooled to room temperature. The solvent was removed under reduced pressure and the residue purified by chromatography (cyclohexane/EtOAc 95:5) to give **13** (375 mg, 0.65 mmol, 65% for two steps) as a colorless oil. ¹H NMR (CDCl₃, 300 MHz) δ 6.69 (dq, J = 9.1, 1.4 Hz, 1H), 4.32 (dd, J = 9.2, 2.8 Hz, 1H), 4.20 (q, J = 7.1 Hz, 2H), 3.96 (m, 1H), 3.88 (dt, J = 7.8, 2.9 Hz, 1H), 1.87 (d, J = 1.4 Hz, 3H), 1.56 (ddd, J = 14.1, 8.6, 3.1 Hz, 1H), 1.38 (ddd, J = 14.1, 8.3, 3.8 Hz, 1H), 1.30 (t, J = 7.1 Hz, 3H), 1.15 (d, J = 6.2 Hz, 3H), 0.89 (s, 18H), 0.87 (s, 9H), 0.12 (s, 3H), 0.09 (s, 3H), 0.07 (s, 3H), 0.06 (s, 3H), 0.04 (s, 3H), 0.01 (s, 3H). ¹³C NMR (CDCl₃, 100 MHz) δ 167.9, 141.8, 127.4, 74.4, 74.3, 66.0, 60.6, 44.8, 26.0 (3C), 25.92 (3C), 25.88 (3C), 24.9, 18.3, 18.2, 18.0, 14.2, 13.4, -3.3, -3.7, -4.2, -4.3, -4.5, -4.8. HRMS-

ESI calculated for C₂₉H₆₂O₅NaSi₃: m/z 597.3803 ([M + Na]⁺). Found: m/z 597.3807 ([M + Na]⁺). [α]_D²⁰ +4.4 (c 0.4, CHCl₃).

(1E,3E)-(5R,6S,8S)-Tris((tert-butylidimethylsilyloxy)-1-iodo-3-methylnona-1,3-diene (14). To a stirred solution of **13** (375 mg, 0.65 mmol) in dry DCM (4.0 mL), under a nitrogen atmosphere, was added DIBAL-H (0.95 mL, 1.5 M in toluene, 1.43 mmol, 2.2 equiv) at 0 °C. The reaction mixture was stirred at 0 °C for 1 h. Saturated aqueous Rochelle salt solution was then added and the resulting mixture warmed to room temperature and vigorously stirred overnight. The aqueous layer was extracted with Et₂O, and the combined organic extracts were washed with water, brine, dried over MgSO₄, filtered and concentrated under reduced pressure. The crude reaction mixture was purified by chromatography (cyclohexane/EtOAc 9:1) to afford (4R,5S,7S,E)-4,5,7-tris((tert-butylidimethylsilyloxy)-2-methyloct-2-en-1-ol (338 mg, 0.63 mmol, 97%) as a colorless oil. ¹H NMR (CDCl₃, 300 MHz) δ 5.45 (dq, J = 8.9, 1.2 Hz, 1H), 4.27 (dd, J = 8.8, 2.6 Hz, 1H), 4.02 (s, 2H), 3.96 (m, 1H), 3.83 (dt, J = 7.7, 2.8 Hz, 1H), 1.71 (d, J = 1.2 Hz, 3H), 1.54 (ddd, J = 14.1, 8.6, 3.1 Hz, 1H), 1.37 (ddd, J = 14.1, 7.9, 3.4 Hz, 1H), 1.15 (d, J = 6.2 Hz, 3H), 0.89 (s, 9H), 0.89 (s, 9H), 0.88 (s, 9H), 0.11 (s, 3H), 0.09 (s, 3H), 0.07 (s, 6H), 0.04 (s, 3H), 0.01 (s, 3H). ¹³C NMR (CDCl₃, 100 MHz) δ 135.4, 126.6, 74.7, 73.7, 68.7, 66.2, 44.7, 26.1 (3C), 26.0 (3C), 25.9 (3C), 25.0, 18.3, 18.2, 18.0, 14.5, -3.2, -3.5, -4.1, -4.3, -4.5, -4.6. HRMS-ESI calculated for C₂₇H₆₀O₄NaSi₃: m/z 555.3697 ([M + Na]⁺). Found: m/z 555.3699 ([M + Na]⁺). [α]_D²⁰ +12.3 (c 1.0, CHCl₃).

To a stirred solution of the latter alcohol (338 mg, 0.63 mmol) in dry DCM (6.3 mL) under a nitrogen atmosphere was added MnO₂ (830 mg, 9.52 mmol, 15 equiv) at room temperature. The reaction mixture was warmed to 40 °C and vigorously stirred for 48 h. The resulting mixture was cooled to room temperature and filtered through Celite with DCM. The solvent was then removed under reduced pressure to give (4R,5S,7S,E)-4,5,7-tris((tert-butylidimethylsilyloxy)-2-methyloct-2-enal (265 mg, 0.50 mmol, 79%) as a colorless oil which was used in the next step without further purification. ¹H NMR (CDCl₃, 300 MHz) δ 9.45 (s, 1H), 6.44 (dq, J = 8.9, 1.4 Hz, 1H), 4.49 (dd, J = 8.9, 2.6 Hz, 1H), 3.99–3.93 (2H), 1.80 (d, J = 1.4 Hz, 3H),

1.51 (ddd, $J = 14.1, 8.9, 3.0$ Hz, 1H), 1.36 (ddd, $J = 14.1, 7.9, 3.0$ Hz, 1H), 1.15 (d, $J = 6.2$ Hz, 3H), 0.89 (s, 18H), 0.87 (s, 9H), 0.14 (s, 3H), 0.11 (s, 3H), 0.07 (s, 6H), 0.05 (s, 3H), 0.01 (s, 3H).

To a stirred solution of CrCl_2 (368 mg, 3.00 mmol, 6 equiv) in dry THF (3.0 mL), under a nitrogen atmosphere, was added a solution of (4*R*,5*S*,7*S*,*E*)-4,5,7-tris((*tert*-butyldimethylsilyloxy)-2-methyloct-2-enal (265 mg, 0.50 mmol) and CHI_3 (590 mg, 1.49 mmol, 3 equiv) in dry THF (2.1 mL) dropwise. The reaction mixture was stirred at room temperature for 12 h. The resulting mixture was hydrolyzed with water and diluted with Et_2O . The aqueous layer was extracted three times with Et_2O and the combined organic extracts were washed with water, brine, dried over MgSO_4 , filtered, and concentrated under reduced pressure. The crude product was then purified by chromatography (cyclohexane/toluene 100:1) to afford **14** (250 mg, 0.38 mmol, 75%) as a pale yellow oil. ^1H NMR (C_6D_6 , 300 MHz) δ 7.05 (d, $J = 14.1$ Hz, 1H), 6.01 (d, $J = 14.1$ Hz, 1H), 5.56 (dq, $J = 9.1, 1.2$ Hz, 1H), 4.40 (dd, $J = 9.1, 2.8$ Hz, 1H), 4.12 (m, 1H), 4.05 (dt, $J = 7.8, 2.8$ Hz, 1H), 1.69 (ddd, $J = 14.1, 8.9, 2.8$ Hz, 1H), 1.57 (ddd, $J = 14.1, 7.9, 2.9$ Hz, 1H), 1.47 (d, $J = 1.2$ Hz, 3H), 1.13 (d, $J = 6.2$ Hz, 3H), 1.03 (s, 9H), 1.00 (s, 18H), 0.25 (s, 3H), 0.23 (s, 3H), 0.14 (s, 3H), 0.11 (s, 3H), 0.10 (s, 3H), 0.06 (s, 3H). ^{13}C NMR (C_6D_6 , 100 MHz) δ 149.6, 135.0, 134.6, 76.6, 75.4, 74.7, 66.9, 45.7, 26.7 (3C), 26.6 (3C), 26.5 (3C), 25.6, 19.0, 18.9, 18.7, 13.1, -2.6, -2.8, -3.6, -3.7, -3.9, -4.1.

(1*E*,3*E*)-(5*R*,6*S*,8*S*)-Tris(*tert*-butyldimethylsilyloxy)-1-tributylstannyl-3-methylnona-1,3-diene (15a). To a stirred solution of **14** (250 mg, 0.38 mmol) in dry Et_2O (2.0 mL), under a nitrogen atmosphere, was added *n*-BuLi (0.17 mL, 2 M in hexane, 0.57 mmol, 1.5 equiv) at -78°C . The reaction mixture was stirred for 20 min at -78°C , and Bu_3SnCl (0.17 mL, 0.57 mmol, 1.5 equiv) was added. The resulting solution was stirred at -78°C for another 20 min and allowed to warm to room temperature for 1 h. Saturated aqueous NaHCO_3 solution was then added, and the aqueous layer was extracted three times with Et_2O . The combined organic extracts were washed with brine, dried over MgSO_4 , filtered, and concentrated under reduced pressure. The crude **15a** was used in the next step without further purification.

(2*E*,4*E*,6*E*,8*E*,10*E*,12*R*,13*S*,15*S*)-Ethyl 12,13,15-Tris((*tert*-butyldimethylsilyloxy)-4,6,10-trimethylhexadeca-2,4,6,8,10-pentaenoate (17). To a stirred solution of crude **15a** and tetra-*n*-butylammonium diphenylphosphinate (415 mg, 0.89 mmol, 2.3 equiv) in dry NMP (2.7 mL), under a nitrogen atmosphere, was added 0.2 mL of a solution of **16**³³ (240 mg, 0.77 mmol, 2 equiv) in NMP (1.8 mL). After addition of copper thiophenecarboxylate (150 mg, 0.77 mmol, 2 equiv), the rest of the **16** solution was added dropwise, and the resulting mixture was stirred at room temperature for 40 min. The reaction mixture was then diluted with Et_2O and filtered through neutral alumina oxide. The filtrate was washed with water, brine, dried over MgSO_4 , filtered, and concentrated under reduced pressure. The crude product was then purified by preparative TLC (cyclohexane/ EtOAc 9:1) to afford **17** (120 mg, 0.17 mmol, 45% for two steps) as a yellow oil. NMR analysis showed the presence of a mixture of isomers 4'*E*/4'*Z* = 93:7. ^1H NMR (CDCl_3 , 300 MHz, 4'*E* isomer) δ 7.95 (d, $J = 15.3$ Hz, 1H, *Z* isomer), 7.38 (d, $J = 15.5$ Hz, 1H, *E* isomer), 6.50 (dd, $J = 14.9, 11.1$ Hz, 1H), 6.37 (d, $J = 14.9$ Hz, 1H), 6.36 (s, 1H), 6.27 (d, $J = 11.1$ Hz, 1H), 5.87 (d, $J = 15.5$ Hz, 1H), 5.57 (d, $J = 9.1$ Hz, 1H), 4.35 (dd, $J = 9.1, 2.8$ Hz, 1H), 4.23 (q, $J = 7.1$ Hz, 2H), 3.96 (m, 1H), 3.87 (dt, $J = 7.6, 2.9$ Hz, 1H), 2.06 (s, 3H), 2.03 (s, 3H), 1.85 (s, 3H), 1.53 (m, 1H), 1.36 (m, 1H), 1.32 (t, $J = 7.1$ Hz, 3H), 1.14 (d, $J = 6.1$ Hz, 3H), 0.89 (s, 9H), 0.88 (s, 9H), 0.87 (s, 9H), 0.11 (s, 3H), 0.09 (s, 3H), 0.08 (s, 3H), 0.06 (s, 3H), 0.03 (s, 3H), 0.00 (s, 3H). ^{13}C NMR (CDCl_3 , 100 MHz, 4'*E* isomer) δ 167.5, 150.7, 143.7, 139.7, 135.1, 134.7, 134.0, 133.9, 132.2, 123.7, 116.1, 74.8, 74.1, 66.2, 60.2, 44.9, 26.1 (3C), 26.0 (3C), 25.9 (3C), 25.0, 18.33, 18.27, 18.0, 17.1, 14.3, 14.2, 13.4, -3.3, -3.5, -4.2, -4.3, -4.6, -4.7.

(2*E*,4*E*,6*E*,8*E*,10*E*,12*R*,13*S*,15*S*)-12,13,15-Tris((*tert*-butyldimethylsilyloxy)-4,6,10-trimethylhexadeca-2,4,6,8,10-pentaenoic Acid (18a). To a stirred solution of **17** (117 mg, 0.16 mmol) in a mixture THF/MeOH/ H_2O (3.5/0.9/0.9 mL) was added LiOH (40 mg, 1.65 mmol, 10 equiv). The resulting mixture was stirred at room temperature for 18 h. After addition of a saturated aqueous

NH_4Cl solution, the mixture was extracted three times with EtOAc and the combined organic extracts were washed with brine, dried over MgSO_4 , filtered, and concentrated under reduced pressure. The crude material was purified by preparative TLC (cyclohexane/ EtOAc 7:3) to afford **18a** (72 mg, 0.11 mmol, 64%) as a yellow oil. NMR analysis showed the presence of mixture of isomers 4'*E*/4'*Z* = 85:15. ^1H NMR (acetone- d_6 , 300 MHz, 4'*E* isomer) δ 7.93 (d, $J = 15.5$ Hz, 1H, *Z* isomer), 7.35 (d, $J = 15.6$ Hz, 1H, *E* isomer), 6.67 (dd, $J = 15.1, 11.1$ Hz, 1H), 6.46 (d, $J = 15.1$ Hz, 1H), 6.46 (s, 1H), 6.39 (d, $J = 11.1$ Hz, 1H), 5.87 (d, $J = 15.6$ Hz, 1H), 5.63 (d, $J = 9.1$ Hz, 1H), 4.49 (dd, $J = 9.1, 2.8$ Hz, 1H), 4.06 (m, 1H), 3.97 (dt, $J = 7.6, 2.9$ Hz, 1H), 2.09 (s, 3H), 2.06 (s, 3H), 1.93 (s, 3H), 1.64 (ddd, $J = 14.1, 8.8, 3.1$ Hz, 1H), 1.41 (ddd, $J = 14.1, 7.7, 3.2$ Hz, 1H), 1.17 (d, $J = 6.2$ Hz, 3H), 0.91 (s, 18H), 0.89 (s, 9H), 0.17 (s, 3H), 0.15 (s, 3H), 0.11 (s, 3H), 0.10 (s, 3H), 0.09 (s, 3H), 0.05 (s, 3H). ^{13}C NMR (acetone- d_6 , 100 MHz, 4'*E* isomer) δ 168.1, 151.6, 144.3, 140.3, 136.2, 135.5, 135.4, 135.0, 133.3, 125.3, 117.3, 75.9, 75.2, 67.1, 45.8, 26.6 (3C), 26.5 (3C), 26.4 (3C), 25.5, 19.0, 18.9, 18.7, 17.2, 14.4, 13.9, -2.9, -3.0, -3.7, -3.8, -4.1, -4.3. HRMS-ESI calculated for $\text{C}_{37}\text{H}_{70}\text{O}_5\text{NaSi}_3$: m/z 701.4423 ($[\text{M} + \text{Na}]^+$). Found: m/z 701.4423 ($[\text{M} + \text{Na}]^+$).

(6*S*,7*S*,9*E*,12*R*)-7-Methyl-2-oxo-12-(propan-2-yl)-1-oxacyclododec-9-en-6-yl-(2*E*,4*E*,6*E*,8*E*,10*E*,12*R*,13*S*,15*S*)-12,13,15-trihydroxy-4,6,10-trimethylhexadeca-2,4,6,8,10-pentaenoate (5e). To a solution of **18a** (22 mg, 0.03 mmol) in benzene (0.4 mL) were added diisopropylethylamine (23 μL , 0.12 mmol, 6 equiv), 2,4,6-trichlorobenzoyl chloride (11 μL , 0.06 mmol, 3 equiv), and DMAP (20 mg). The reaction mixture was stirred at room temperature for 15 min, and **5a**³³ (5.5 mg, 0.02 mmol) was added. After being stirred at room temperature for 14 h, an aqueous saturated solution of sodium hydrogenocarbonate was added to the reaction mixture. The aqueous layer was extracted three times with benzene. The combined organic layers were washed with brine, dried over MgSO_4 , filtered, and concentrated under reduced pressure. The crude product was purified on preparative TLC, eluting with heptane/ethyl acetate 90:10 to give (6*S*,7*S*,9*E*,12*R*)-7-methyl-2-oxo-12-(propan-2-yl)-1-oxacyclododec-9-en-6-yl (2*E*,4*E*,6*E*,8*E*,10*E*,12*R*,13*S*,15*S*)-12,13,15-tris[(*tert*-butyldimethylsilyloxy)-4,6,10-trimethylhexadeca-2,4,6,8,10-pentaenoate (13 mg, 0.014 mmol, 71%) as a yellow oil. A (4'*E*)/(4'*Z*) = 61:39 mixture could be detected by ^1H NMR analysis. ^1H NMR (CDCl_3 , 300 MHz) δ 7.93 (d, $J = 15.5$ Hz, 1H, *Z* isomer), 7.36 (d, $J = 15.5$ Hz, 1H, *E* isomer), 6.51 (dd, $J = 14.8, 11.8$ Hz, 1H), 6.37 (d, $J = 14.8$ Hz, 1H), 6.34 (s, 1H), 6.26 (d, $J = 11.8$ Hz, 1H), 5.85 (d, $J = 15.5$ Hz, 1H), 5.56 (d, $J = 9.0$ Hz, 1H), 5.51 (m, 1H), 5.25 (m, 1H), 4.82–4.73 (2H), 4.34 (dd, $J = 2.8, 8.8$ Hz, 1H), 3.94 (m, 1H), 3.86 (td, $J = 2.8, 7.7$ Hz, 1H), 2.49 (m, 1H), 2.30 (m, 1H), 2.14–2.06 (2H), 2.05 (s, 3H), 2.02 (s, 3H), 1.95 (m, 1H), 1.84 (s, 3H), 1.87–1.61 (6H), 1.13 (d, $J = 6.1$ Hz, 3H), 0.94 (s, 3H), 0.93 (s, 3H), 0.91 (s, 3H), 0.90 (s, 3H), 0.88 (s, 9H), 0.87 (s, 9H), 0.86 (s, 9H), 0.10 (s, 3H), 0.08 (s, 3H), 0.05 (s, 6H), 0.02 (s, 3H), -0.01 (s, 3H).

To a solution of the latter compound (13 mg, 0.015 mmol) in THF (0.1 mL) was added TBAF (0.130 mmol, 1 M in THF, 9 equiv), and the solution was stirred at room temperature for 4 h. CaCO_3 (40 mg), Dowex 50WX8-400 (110 mg), and MeOH (0.3 mL) were added, and the reaction mixture was stirred for 1 h. After being filtered and concentrated under reduced pressure, the crude product was purified by preparative TLC ($\text{CH}_2\text{Cl}_2/\text{MeOH}$ 90:10) to give **5e** (6 mg, 0.01 mmol, 67%). A (4'*E*)/(4'*Z*) = 56:44 mixture could be detected by ^1H NMR analysis. ^1H NMR (acetone- d_6 , 400 MHz) δ 7.93 (d, $J = 15.6$ Hz, 1H, *Z* isomer), 7.37 (d, $J = 15.5$ Hz, 1H, *E* isomer), 6.63 (dd, $J = 11.1, 15.0$ Hz, 1H), 6.47 (s, 1H), 6.36 (d, $J = 15.0$ Hz, 1H), 6.17 (d, $J = 11.1$ Hz, 1H), 5.89 (d, $J = 15.5$ Hz, 1H), 5.68 (d, $J = 8.5$ Hz, 1H), 5.50 (m, 1H), 5.30 (m, 1H), 4.78–4.67 (2H), 4.38 (m, 1H), 4.04 (m, 1H), 3.88 (m, 1H), 3.81 (m, 1H), 3.69 (m, 1H), 3.63 (m, 1H), 2.49 (m, 1H), 2.32 (m, 1H), 2.12–2.08 (2H), 2.06 (s, 3H), 1.97 (s, 3H), 1.95–1.92 (2H), 1.90 (s, 3H), 1.80–1.75 (4H), 1.70–1.62 (2H), 1.54–1.49 (2H), 1.13 (d, $J = 6.1$ Hz, 3H), 0.92 (s, 3H), 0.90 (s, 3H), 0.87 (s, 3H). ^{13}C NMR (acetone- d_6 , 100 MHz) δ 173.9, 167.8, 152.2, 144.1, 141.6, 137.3, 136.5, 136.1, 134.1, 133.0, 128.0, 125.8, 120.6, 118.4, 80.2, 77.3, 73.5, 73.3, 65.9, 43.1, 39.8, 37.9, 37.0, 36.1, 34.1, 25.6, 22.0, 21.6, 20.9, 19.9, 19.4, 18.1, 15.3, 14.3. HRMS-ESI calculated for

C₃₄H₅₂O₇Na: *m/z* 595.3605 ([M + Na]⁺). Found: *m/z* 595.3600 ([M + Na]⁺).

Biological Procedures. Natural Mycolactones. Mycolactone (A/B form) was purified from *M. ulcerans* 1615 (ATCC 35840).⁷ A biologically active, biotin-bearing derivative of mycolactone A/B was prepared as described.¹⁴ The concentration and purity of all mycolactone preparations were assessed by HPLC–MS/MS. Stock solutions in dimethyl sulfoxide (DMSO) were conserved at –20 °C, protected from light. They were diluted >1000 times in culture medium extemporaneously and compared to vehicle-treated controls in bioassays.

WASP/N-WASP Constructs. GST-fused MBDs corresponding to the MBD in WASP (200–313) or N-WASP (186–276) and His₆-tagged VCA constructs were expressed and purified as described.¹⁴

ELISAs. The binding of each mycolactone variant to WASP/N-WASP was measured indirectly, through their capacity to displace biotinylated mycolactone from immobilized MBDs.¹⁴ Briefly, GST-fused MBDs (5 μg/mL) in PBS were coated onto plastic 96 microtiter wells (NUNC MaxiSorp) by overnight incubation at 4 °C. After a 1 h blocking step at room temperature with PBS + 1% bovine serum albumin (BSA), plates were washed with PBS + 0.05% Tween20 and incubated for 2 h at room temperature with biotinylated mycolactone (1 μM) plus increasing amounts of mycolactone variants (0–10 μM) in PBS + 0.1% BSA. After washing, complexes were revealed by addition of streptavidin-conjugated alkaline phosphatase (1 h, room temperature) and colorimetric detection.

VCA Displacement Assay. The capacity of **5b** to displace VCA from the MBD in WASP or N-WASP was adapted from the procedure used to indicate mycolactone dissociating activity.¹⁴ Briefly, GST-fused MBD was immobilized on glutathione-sepharose beads and then incubated with His₆-tagged VCA in the presence of increasing amounts of **5b**. After thorough washing of the beads, bound products were analyzed by gel electrophoresis and silver staining.

Epithelial Cell Adhesion Assay. Background of the E-plates was determined in 50 μL cell culture medium prior to addition of 150 μL of HeLa cell suspension (20 000 cells/well). Plates were then placed into the real-time cell analyzer (RTCA) station, and impedance was measured every 15 min. Impedance values are represented by cell index (CI) values ((Z_i – Z₀) [Ω]/15 [Ω]); Z₀ is background resistance, and Z_i is individual time point resistance).

■ ASSOCIATED CONTENT

● Supporting Information

Experimental procedures and NMR spectra. This material is available free of charge via the Internet at <http://pubs.acs.org>.

■ AUTHOR INFORMATION

Corresponding Authors

*A.-C. C.: phone, +33 3 8933 6855; fax, +33 3 8933 6860; e-mail, chanyac@gmail.com.

*N. B.: phone, +33 3 8933 6824; fax, +33 3 8933 6860; e-mail, n.blanchard@unistra.fr.

Author Contributions

The manuscript was written through contributions of all authors. All authors have given approval to the final version of the manuscript.

Notes

The authors declare no competing financial interest.

■ ACKNOWLEDGMENTS

We thank Sandrine Vitry (Institut Pasteur, Paris, France) for helping us with the XCelligence assays of epithelial cell adhesion. This work received financial support from the “Association Raoul Follereau”, the “Fondation pour la Recherche Médicale, Equipes FRM 2012, Project DEQ20120323704”, the “Region Ile de France”, the CNRS,

the University of Haute-Alsace, and the University of Strasbourg.

■ ABBREVIATIONS USED

Arp, actin-related protein; AT2R, angiotensin II receptor; CPE, cytopathic effect; CRIB, Cdc42/Rac-interactive-binding; CuTC, copper thiophenecarboxylate; HKR, hydrolytic kinetic resolution; MBD, mycolactone binding domain; N-WASP, neural Wiskott–Aldrich syndrome protein; TEMPO, 2,2,6,6-tetramethylpiperidine 1-oxyl; VCA, verprolin-cofilin-acidic; WASP, Wiskott–Aldrich syndrome protein

■ REFERENCES

- (1) O'Brien, D. P.; Comte, E.; Serafini, M.; Ehounou, G.; Antierens, A.; Vuagnat, H.; Christinet, V.; Hamani, M. D.; du Cros, P. The urgent need for clinical, diagnostic, and operational research for management of Buruli ulcer in Africa. *Lancet Infect. Dis.* **2014**, *14*, 435–440.
- (2) Chany, A.-C.; Tresse, C.; Casarotto, V.; Blanchard, N. History, biology and chemistry of *Mycobacterium ulcerans* infections (Buruli ulcer disease). *Nat. Prod. Rep.* **2013**, *30*, 1527–1567.
- (3) Walsh, D. S.; Portaels, F.; Meyers, W. M. Buruli ulcer (*Mycobacterium ulcerans* infection): a re-emerging disease. *Clin. Microbiol. Newsl.* **2009**, *31*, 119–127.
- (4) Demangel, C.; Stinear, T. P.; Cole, S. T. Buruli ulcer: reductive evolution enhances pathogenicity of *Mycobacterium ulcerans*. *Nat. Rev. Microbiol.* **2009**, *7*, 50–60.
- (5) Hong, H.; Demangel, C.; Pidot, S. J.; Leadlay, P. F.; Stinear, T. Mycolactones: immunosuppressive and cytotoxic polyketides produced by aquatic mycobacteria. *Nat. Prod. Rep.* **2008**, *25*, 447–454.
- (6) MacCallum, P.; Tolhurst, J. C.; Buckle, G.; Sissons, H. A. A new mycobacterial infection in man. *J. Pathol. Bacteriol.* **1948**, *60*, 93–122.
- (7) George, K. M.; Chatterjee, D.; Gunawardana, G.; Welty, D.; Hayman, J.; Lee, R.; Small, P. L. C. Mycolactone: a polyketide toxin from *Mycobacterium ulcerans* required for virulence. *Science* **1999**, *283*, 854–857.
- (8) Gunawardana, G.; Chatterjee, D.; George, K. M.; Brennan, P.; Whittorn, D.; Small, P. L. C. Characterization of novel macrolide toxins, mycolactones A and B, from a human pathogen, *Mycobacterium ulcerans*. *J. Am. Chem. Soc.* **1999**, *121*, 6092–6093.
- (9) Kishi, Y. Chemistry of mycolactones, the causative toxins of Buruli ulcer. *Proc. Natl. Acad. Sci. U.S.A.* **2011**, *108*, 6703–6708.
- (10) Song, F. B.; Fidanze, S.; Benowitz, A. B.; Kishi, Y. Total synthesis of the mycolactones. *Org. Lett.* **2002**, *4*, 647–650.
- (11) Fidanze, S.; Song, F. B.; Szlosek-Pinaud, M.; Small, P. L. C.; Kishi, Y. Complete structure of the mycolactones. *J. Am. Chem. Soc.* **2001**, *123*, 10117–10118.
- (12) Benowitz, A. B.; Fidanze, S.; Small, P. L. C.; Kishi, Y. Stereochemistry of the core structure of the mycolactones. *J. Am. Chem. Soc.* **2001**, *123*, 5128–5129.
- (13) Guenin-Macé, L.; Oldenburg, R.; Chrétien, F.; Demangel, C. Pathogenesis of skin ulcers: lessons from the *Mycobacterium ulcerans* and *Leishmania* spp. pathogens. *Cell. Mol. Life Sci.* **2014**, *71*, 2443–2450.
- (14) Guenin-Macé, L.; Veyron-Churlet, R.; Thoulouze, M. I.; Romet-Lemonne, G.; Hong, H.; Leadlay, P. F.; Danckaert, A.; Ruf, M. T.; Mostowy, S.; Zurzolo, C.; Bousso, P.; Chretien, F.; Carlier, M. F.; Demangel, C. Mycolactone activation of Wiskott–Aldrich syndrome proteins underpins Buruli ulcer formation. *J. Clin. Invest.* **2013**, *123*, 1501–1512.
- (15) Thrasher, A. J.; Burns, S. O. WASP: a key immunological multitasker. *Nat. Rev. Immunol.* **2010**, *10*, 182–192.
- (16) Boulkroun, S.; Guenin-Macé, L.; Thoulouze, M. I.; Monot, M.; Merckx, A.; Langsley, G.; Bismuth, G.; Di Bartolo, V.; Demangel, C. Mycolactone suppresses T cell responsiveness by altering both early signaling and posttranslational events. *J. Immunol.* **2010**, *184*, 1436–1444.

- (17) Coutanceau, E.; Decalf, J.; Martino, A.; Babon, A.; Winter, N.; Cole, S. T.; Albert, M. L.; Demangel, C. Selective suppression of dendritic cell functions by *Mycobacterium ulcerans* toxin mycolactone. *J. Exp. Med.* **2007**, *204*, 1395–1403.
- (18) Coutanceau, E.; Marsollier, L.; Brosch, R.; Perret, E.; Goossens, P.; Tanguy, M.; Cole, S. T.; Small, P. L. C.; Demangel, C. Modulation of the host immune response by a transient intracellular stage of *Mycobacterium ulcerans*: the contribution of endogenous mycolactone toxin. *Cell Microbiol.* **2005**, *7*, 1187–1196.
- (19) Guenin-Macé, L.; Carrette, F.; Asperti-Boursin, F.; Le Bon, A.; Caleechurn, L.; Di Bartolo, V.; Fontanet, A.; Bismuth, G.; Demangel, C. Mycolactone impairs T cell homing by suppressing microRNA control of L-selectin expression. *Proc. Natl. Acad. Sci. U.S.A.* **2011**, *108*, 12833–12838.
- (20) Hall, B.; Simmonds, R. Pleiotropic molecular effects of the *Mycobacterium ulcerans* virulence factor mycolactone underlying the cell death and immunosuppression seen in Buruli ulcer. *Biochem. Soc. Trans.* **2014**, *42*, 177–183.
- (21) Hall, B. S.; Hill, K.; McKenna, M.; Ogbuchi, J.; High, S.; Willis, A. E.; Simmonds, R. E. The pathogenic mechanism of the *Mycobacterium ulcerans* virulence factor, mycolactone, depends on blockade of protein translocation into the ER. *PLoS Pathog.* **2014**, *10*, e1004061.
- (22) Pahlevan, A. A.; Wright, D. J. M.; Andrews, C.; George, K. M.; Small, P. L. C.; Foxwell, B. M. The inhibitory action of *Mycobacterium ulcerans* soluble factor on monocyte/T cell cytokine production and NF-kappa B function. *J. Immunol.* **1999**, *163*, 3928–3935.
- (23) Simmonds, R. E.; Lali, F. V.; Smallie, T.; Small, P. L. C.; Foxwell, B. M. Mycolactone inhibits monocyte cytokine production by a posttranscriptional mechanism. *J. Immunol.* **2009**, *182*, 2194–2202.
- (24) Marion, E.; Song, O.-R.; Christophe, T.; Babonneau, J.; Fenistein, D.; Eyer, J.; Letournel, F.; Henrion, D.; Clere, N.; Paille, V.; Guérineau, N. C.; Saint André, J.-P.; Gersbach, P.; Altmann, K.-H.; Stinear, T. P.; Comoglio, Y.; Sandoz, G.; Preisser, L.; Delneste, Y.; Yeramian, E.; Marsollier, L.; Brodin, P. Mycobacterial toxin induces analgesia in Buruli ulcer by targeting the angiotensin pathways. *Cell* **2014**, *157*, 1565–1576.
- (25) Danser, A. H. J.; Anand, P. The angiotensin II type 2 receptor for pain control. *Cell* **2014**, *157*, 1504–1506.
- (26) Hande, S. M.; Kazumi, Y.; Lai, W. G.; Jackson, K. L.; Maeda, S.; Kishi, Y. Synthesis and structure of two new mycolactones isolated from *M. ulcerans* subsp. *shinshuense*. *Org. Lett.* **2012**, *14*, 4618–4621.
- (27) Spangenberg, T.; Aubry, S.; Kishi, Y. Synthesis and structure assignment of the minor metabolite arising from the frog pathogen *Mycobacterium liflandii*. *Tetrahedron Lett.* **2010**, *51*, 1782–1785.
- (28) Kim, H. J.; Kishi, Y. Total synthesis and stereochemistry of mycolactone F. *J. Am. Chem. Soc.* **2008**, *130*, 1842–1843.
- (29) Aubry, S.; Lee, R. E.; Mahrous, E. A.; Small, P. L. C.; Beachboard, D.; Kishi, Y. Synthesis and structure of mycolactone E isolated from frog *Mycobacterium*. *Org. Lett.* **2008**, *10*, 5385–5388.
- (30) Judd, T. C.; Bischoff, A.; Kishi, Y.; Adusumilli, S.; Small, P. L. C. Structure determination of mycolactone C via total synthesis. *Org. Lett.* **2004**, *6*, 4901–4904.
- (31) Scherr, N.; Gersbach, P.; Dangy, J.-P.; Bomio, C.; Li, J.; Altmann, K.-H.; Pluschke, G. Structure–activity relationship studies on the macrolide exotoxin mycolactone of *Mycobacterium ulcerans*. *PLoS Neglected Trop. Dis.* **2013**, *7*, e2143.
- (32) Gersbach, P.; Jantsch, A.; Feyen, F.; Scherr, N.; Dangy, J.-P.; Pluschke, G.; Altmann, K.-H. A ring-closing metathesis (RCM)-based approach to mycolactones A/B. *Chem.—Eur. J.* **2011**, *17*, 13017–13031.
- (33) Chany, A.-C.; Casarotto, V.; Schmitt, M.; Tarnus, C.; Guenin-Macé, L.; Demangel, C.; Mirguet, O.; Eustache, J.; Blanchard, N. A diverted total synthesis of mycolactone analogues: an insight into Buruli ulcer toxins. *Chem.—Eur. J.* **2011**, *17*, 14413–14419.
- (34) Analogue **4f** was recently synthesized in our group and for the sake of clarity is directly compared in Figure 2 with **4a–e** that we reported in 2011. **4f** at a concentration of 10 μ M induced the rounding up of 40% of the L929 cells after 48 h (versus 100% of cell rounding with **4b**), demonstrating the relative importance of the C15'-position.
- (35) Ando, K. Highly selective synthesis of Z-unsaturated esters by using new Horner–Emmons reagents, ethyl (diarylphosphono)acetates. *J. Org. Chem.* **1997**, *62*, 1934–1939.
- (36) Ando, K. Practical synthesis of Z-unsaturated esters by using a new Horner–Emmons reagent, ethyl diphenylphosphonoacetate. *Tetrahedron Lett.* **1995**, *36*, 4105–4108.
- (37) Kolb, H. C.; VanNieuwenhze, M. S.; Sharpless, K. B. Catalytic asymmetric dihydroxylation. *Chem. Rev.* **1994**, *94*, 2483–2547.
- (38) Allred, G. D.; Liebeskind, L. S. Copper-mediated cross-coupling of organostannanes with organic iodides at or below room temperature. *J. Am. Chem. Soc.* **1996**, *118*, 2748–2749.
- (39) Donnard, M.; Blanchard, N. Copper-catalyzed C–C bond formation in natural product synthesis: elegant and efficient solutions to a key bond disconnection. In *Copper-Mediated Cross-Coupling Reactions*; John Wiley & Sons, Inc.: Hoboken, NJ, 2013; pp 683–723.
- (40) Evano, G.; Blanchard, N.; Toumi, M. Copper-mediated coupling reactions and their applications in natural products and designed biomolecules synthesis. *Chem. Rev.* **2008**, *108*, 3054–3131.
- (41) Seco, J. M.; Quiñoá, E.; Riguera, R. Assignment of the absolute configuration of polyfunctional compounds by NMR using chiral derivatizing agents. *Chem. Rev.* **2012**, *112*, 4603–4641.
- (42) Freire, F.; Seco, J. M.; Quiñoá, E.; Riguera, R. Determining the absolute stereochemistry of secondary/secondary diols by ¹H NMR: basis and applications. *J. Org. Chem.* **2005**, *70*, 3778–3790.
- (43) Seco, J. M.; Quiñoá, E.; Riguera, R. The assignment of absolute configuration by NMR. *Chem. Rev.* **2004**, *104*, 17–118.
- (44) Ford, D. D.; Nielsen, L. P. C.; Zuend, S. J.; Musgrave, C. B.; Jacobsen, E. N. Mechanistic basis for high stereoselectivity and broad substrate scope in the (salen)Co(III)-catalyzed hydrolytic kinetic resolution. *J. Am. Chem. Soc.* **2013**, *135*, 15595–15608.
- (45) Tokunaga, M.; Larrow, J. F.; Kakiuchi, F.; Jacobsen, E. N. Asymmetric catalysis with water: efficient kinetic resolution of terminal epoxides by means of catalytic hydrolysis. *Science* **1997**, *277*, 936–938.
- (46) Even if stereoisomerically pure southern fragments could be prepared, Negishi has shown that spontaneous isomerization occurred upon deprotection of the C12',C13',C15' stereotriad; see the following: Wang, G. W.; Yin, N.; Negishi, E. Highly stereoselective total synthesis of fully hydroxy-protected mycolactones A and B and their stereoisomerization upon deprotection. *Chem.—Eur. J.* **2011**, *17*, 4118–4130.
- (47) Snyder, D. S.; Small, P. L. C. Uptake and cellular actions of mycolactone, a virulence determinant for *Mycobacterium ulcerans*. *Microb. Pathog.* **2003**, *34*, 91–101.
- (48) Hong, H.; Coutanceau, E.; Leclerc, M.; Caleechurn, L.; Leadlay, P. F.; Demangel, C. Mycolactone diffuses from *Mycobacterium ulcerans*-infected tissues and targets mononuclear cells in peripheral blood and lymphoid organs. *PLoS Neglected Trop. Dis.* **2008**, *2*, e325.